

## Over 10 000 $\delta$ Scuti Stars toward the Galactic Bulge from OGLE-IV\*

P. Pietrukowicz<sup>1</sup>, I. Soszyński<sup>1</sup>, H. Netzel<sup>2</sup>, M. Wrona<sup>1</sup>,  
A. Udalski<sup>1</sup>, M.K. Szymański<sup>1</sup>, R. Poleski<sup>1</sup>, S. Kozłowski<sup>1</sup>,  
J. Skowron<sup>1</sup>, K. Ulaczyk<sup>1,3</sup>, D.M. Skowron<sup>1</sup>, P. Mróz<sup>1,4</sup>,  
K. Rybicki<sup>1</sup>, P. Iwanek<sup>1</sup> and M. Gromadzki<sup>1</sup>

<sup>1</sup>Astronomical Observatory, University of Warsaw, Al. Ujazdowskie 4, 00-478 Warszawa, Poland

<sup>2</sup>Nicolaus Copernicus Astronomical Center, ul. Bartycka 18, 00-716 Warszawa, Poland

<sup>3</sup>Department of Physics, University of Warwick, Coventry CV4 7AL, UK

<sup>4</sup>Division of Physics, Mathematics, and Astronomy, California Institute of Technology, Pasadena, CA 91125, USA

Received December 28, 2020

### ABSTRACT

We present a collection of 10 111 genuine  $\delta$  Sct-type pulsating variable stars detected in the OGLE-IV Galactic bulge fields. In this sample, 9835 variables are new discoveries. For most of the stars photometric data cover the whole decade 2010–2019. We illustrate a huge variety of light curve shapes of  $\delta$  Sct variables. Long-term observations have allowed us to spot objects with evident period, amplitude, and mean brightness variations. Our analysis indicates that about 28% of the stars are single-mode pulsators. Fourteen  $\delta$  Sct stars show additional eclipsing or ellipsoidal binary modulation. We report significant attenuation or even disappearance of the pulsation signal in six sources. The whole set of variables is a mix of objects representing various Milky Way’s populations, with the majority of stars from the Galactic bulge. There are also representatives of the Sagittarius Dwarf Spheroidal Galaxy. Some of the newly detected variables could be SX Phe-type stars residing in globular clusters. The collection, including full *V*- and *I*-band time-series data, is available to the astronomical community from the OGLE On-line Data Archive.

**Key words:** *Catalogs – Stars: variables: delta Scuti – Galaxy: bulge – Galaxies: individual: Sagittarius Dwarf Spheroidal Galaxy*

### 1. Introduction

$\delta$  Sct-type variables are pulsating stars with periods below 0.3 d and *V*-band amplitudes up to 0.9 mag. They pulsate in radial as well as non-radial acoustic modes excited mainly in the  $\kappa$  mechanism (Breger 2000). The majority of  $\delta$  Sct

---

\*Based on observations obtained with the 1.3-m Warsaw telescope at the Las Campanas Observatory operated by the Carnegie Institution for Science.

stars are multiple-mode pulsators. The spectral types of  $\delta$  Sct variables range from A0 to F6 for luminosity classes III (giants), IV (subgiants), and V (dwarfs). In the Hertzsprung–Russell diagram, these pulsating stars lie at the classical instability strip on the main sequence (MS) or are moving from the MS to the giant branch. They can also be found at the pre-MS stage. The stars belong to various populations. Usually,  $\delta$  Sct stars are considered the Population I stars of the flat Milky Way component (the young Galactic disk). Population II analogues or representatives of the Galactic halo and old disk are sometimes classified as SX Phe stars. This type of variables is observed in globular clusters. SX Phe stars are common among blue stragglers in metal-poor clusters, but relatively rare in metal-rich ones. The mass range of  $\delta$  Sct stars depends on the metal content. Population I pulsators cover a range from about  $1.5 M_{\odot}$  to  $2.3 M_{\odot}$  (Murphy *et al.* 2019), while Population II stars from about  $1.0 M_{\odot}$  to  $1.3 M_{\odot}$  (McNamara 2011). Space-based observations have shown that the vast majority of  $\delta$  Sct stars are low-amplitude pulsators ( $< 0.1$  mag) and only about half of them have amplitudes  $> 0.001$  mag and appear to be variable from the ground (Balona and Dziembowski 2011).

The prototype object of the whole class,  $\delta$  Sct itself, was recognized as a star exhibiting radial velocity variations amongst nine 4th magnitude stars observed by Campbell and Wright (1900). It was thought to be a spectroscopic binary system. Much later, results from photometric and spectroscopic observations of this object reported by Fath (1935) and Colacevich (1935), respectively, showed a short variability period of 0.1937 d and small amplitude of the velocity variations of about 8 km/s. The relation between the radial velocity changes and light variations (nearly mirrored phased curves) was identical to those observed in Cepheids. After the discovery of multiple variability in  $\delta$  Sct (Fath 1937, Sterne 1938), it was natural to interpret the behavior of the star in terms of the pulsation theory. So far, six distinct modes in the power spectrum of  $\delta$  Sct have been detected (Templeton *et al.* 1997).

By December 1956, or within two decades from the identification of  $\delta$  Sct as the pulsating star, four variables of this type were discovered: DQ Cep (Walker 1952), CC And (Lindblad and Eggen 1953),  $\rho$  Pup (Eggen 1956a), and  $\delta$  Del (Eggen 1956b). Shortly thereafter, the number of new  $\delta$  Sct stars (often termed dwarf Cepheids in the past) started to increase much faster and reached 636 sources in January 2000, in the catalog prepared by Rodríguez *et al.* (2000).

A truly rapid increase began in the 1990s with the advent of CCD detectors and wide-field photometric surveys. Dozens of  $\delta$  Sct stars were found as by-products from microlensing surveys. The Optical Gravitational Lensing Experiment during its first phase of operation (OGLE-I, years 1992–1995) discovered 53  $\delta$  Sct stars mainly in the area of Baade’s Window of the Galactic bulge (Udalski *et al.* 1994, 1995ab, 1996, 1997). The MAssive Compact Halo Object (MACHO) project reported on the detection of 90  $\delta$  Sct stars toward the bulge, 86 of which were new variables (Alcock *et al.* 2000). Extensive time-series observations of Galactic globular clusters led to the discovery of tens of SX Phe-type stars (*e.g.*, Kaluzny *et al.*

1996, Pych *et al.* 2001, Mazur *et al.* 2003). In their catalog, Rodríguez and López-González (2000) list 149 such variables belonging to eighteen globular clusters and two nearby galaxies (Carina and Sagittarius Dwarf Spheroidal Galaxies). Pigulski *et al.* (2006) analyzed OGLE-II photometry (collected in years 1997–2000) and reported on the detection of 193 high-amplitude  $\delta$  Sct stars, including 50 multi-periodic objects. In OGLE-III data (years 2001–2009) for the Large Magellanic Cloud, Poleski *et al.* (2010) found 2786 short-period variables, 92 of which were multi-mode pulsators.

Large-scale surveys have multiplied the number of known Galactic  $\delta$  Sct stars. The All-Sky Automated Survey (ASAS, Pojmański 2002) led to the detection of 525 previously unknown  $\delta$  Sct objects. The fifth edition of the General Catalogue of Variable Stars (GCVS, Samus *et al.* 2017, version from November 2020) contains 1019 positions classified as  $\delta$  Sct (DSCT) and 228 positions classified as SX Phe stars (SXPHE). A compiled catalog of 1578 Galactic  $\delta$  Sct pulsators was presented by Chang *et al.* (2013). There were 4514 DSCT and 7 SXPHE identifications in the International Variable Star Index (VSX, Watson *et al.* 2006) in May 2019. Very recently, Jayasinghe *et al.* (2020) presented an all-sky catalog of 8418  $\delta$  Sct variables from the All-Sky Automated Survey for SuperNovae (ASAS-SN, Shappee *et al.* 2014, Kochanek *et al.* 2017). According to the authors, the catalog includes 3322 new discoveries. Finally, Chen *et al.* (2020) published a set of periodic variable stars containing 15 396 candidate  $\delta$  Sct pulsators detected mostly in the northern hemisphere ( $\delta > -25^\circ$ ) by the Zwicky Transient Facility (ZTF, Bellm *et al.* 2019).

$\delta$  Sct stars were intensively observed by Kepler space telescope. A thorough search for such variables was recently carried out by Murphy *et al.* (2019). They identified 1988 genuine  $\delta$  Sct pulsators in the original 105 deg<sup>2</sup> Kepler field monitored for four years almost continuously (from May 2009 to May 2013). Currently, among millions of stellar sources,  $\delta$  Sct stars are observed by Gaia and TESS space missions.

Here, we introduce a collection of 10 111 genuine  $\delta$  Sct variable stars detected in the OGLE-IV Galactic bulge fields. We cross-match our collection with previously published catalogs, including lists of variable stars in globular clusters. In the entire sample, 9835 objects are newly discovered variables. This release significantly increases the number of known  $\delta$  Sct stars in the whole sky. In the paper, we present some general observational properties of the variables and a huge diversity of their light curves.

## 2. OGLE Observations and Data Reductions

The photometric data used in this work were collected with the 1.3-m Warsaw telescope at Las Campanas Observatory (LCO), Chile, during the fourth phase of the OGLE project (OGLE-IV) in years 2010–2019. LCO is operated by the Carnegie Institution for Science. The OGLE-IV mosaic camera consists of 32

$2k \times 4k$  CCD detectors covering a total field of view of  $1.4 \text{ deg}^2$  at a scale of  $0.26 \text{ arcsec/pixel}$ . OGLE monitors optical variability in the area of the Galactic bulge, Galactic disk, and Magellanic System. A total of about 710 000 exposures were collected over the mentioned decade. Around 94% of the frames were taken through the Cousins  $I$  filter. The remaining 6% of the frames were taken through the Johnson  $V$  filter. Details on the instrumentation setup can be found in Udalski *et al.* (2015).

The presented collection of  $\delta$  Sct stars is based on observations of 121 OGLE-IV Galactic bulge fields covering an area of approximately  $172 \text{ deg}^2$ . Seven of the fields are located in the central part of the tidally disrupted Sagittarius Dwarf Spheroidal Galaxy (Sgr dSph). A total number of about 181 500  $I$ -band exposures with the integration time of 100 s (150 s in the case of Sgr dSph) and 6400  $V$ -band exposures with 150 s were obtained. The fields were monitored with various cadence depending mainly on the frequency of microlensing events (Udalski *et al.* 2015). In the most crowded fields, such as BLG501, BLG505, and BLG512, one exposure was taken every 19 min. In general, the number of  $I$ -band measurements varies from 61 up to 16 799 per field, with a median value of 606. In the  $V$  band, there are from several up to 230 observations. Some of the fields were not observed for the whole decade. The least crowded fields, including fields close to the Galactic plane, were monitored in the first 1–4 seasons only. The investigated bulge area contains a total number of  $\approx 4.0 \times 10^8$  stars with brightness between  $I \approx 12.5 \text{ mag}$  and  $I \approx 21.5 \text{ mag}$ . The photometry was obtained with the standard OGLE data reduction pipeline using the Difference Image Analysis (DIA, Alard and Lupton 1998, Woźniak 2000).

In the first step, we carried out a frequency search up to  $100 \text{ d}^{-1}$  with the help of the FNPEAKS code<sup>†</sup> for all  $I$ -band light curves from seasons 2010–2013. It calculates Fourier amplitude spectra of unequally spaced time-series data. The code reduces the computation time for a discrete Fourier transform by co-adding correctly phased, low-resolution Fourier transforms of pieces of the large data set interpolated to high resolution.

In the next step, light curves with high variability signal-to-noise ratio (over 10) were visually inspected. Objects with asymmetric light curves and periods shorter than 0.3 d, excluding evident exceptions, were classified as  $\delta$  Sct candidates. Based on our long-term experience in the field of variable stars, we were able to recognize and separate from the sample objects such as RRc variables (Soszyński *et al.* 2014), blue large-amplitude pulsators (BLAPs; Pietrukowicz *et al.* 2017), eclipsing and ellipsoidal contact binary systems (Soszyński *et al.* 2016).

The initially selected sample required a removal of outlying points from the light curves. For objects with less than 1000  $I$ -band measurements the outliers were removed manually. In the case of objects with more observations, which constitute about 57% of all stars, we applied a  $3\sigma$ -clipping procedure to phased

---

<sup>†</sup><http://helas.astro.uni.wroc.pl/deliverables.php?lang=en&active=fnpeaks>

light curves. After cleaning the data, we improved the periods and re-inspected the whole sample visually. The most interesting examples of  $\delta$  Sct light curves were selected and they are presented in Section 5. The period values were corrected with the TATRY code (Schwarzenberg-Czerny 1996) based on the entire available time span (2010–2019). This code employs periodic orthogonal polynomials to fit the data and the analysis of variance (ANOVA) statistic to evaluate the quality of the fit.

During the inspection, we noticed that many  $\delta$  Sct light curves show a scatter characteristic for multi-mode pulsators. We performed a pre-whitening of the data and we looked for secondary periods. We found 2880 single-mode pulsators. This constitutes about 28% of the whole sample. Searching for and detailed analysis of additional periodicities is the topic of the work by Netzel *et al.* (in preparation). Here, we present several examples of double-mode  $\delta$  Sct stars and candidates for members of binary systems.

Finally, each light curve was calibrated from the instrumental to the standard magnitudes according to the prescription given in Udalski *et al.* (2015). The accuracy of the calibration reaches 0.02 mag in the Johnson-Cousins system. For about 5% of the variables, located mainly in highly-extincted regions, there is no *V*-band measurement. In this case, the *I*-band magnitudes are accurate to 0.05 mag.

Completeness of our search for  $\delta$  Sct variables depends on brightness and amplitude of the stars. Precise long-term observations conducted from the ground allow for a very effective detection of high-amplitude  $\delta$  Sct stars (HADS, *V*-band amplitudes  $> 0.15$  mag or *I*-band amplitudes  $> 0.1$  mag). As we show in Section 4, our search is highly complete for variables brighter than 17.5 mag and with amplitudes higher than 0.1 mag in the *I* band. Completeness of the search for bright HADS is similar to the completeness for RRab type stars, that is of about 97% (Soszyński *et al.* 2014).

### 3. The Collection

The OGLE collection of  $\delta$  Sct-type variable stars in the Galactic bulge fields contains 10 111 objects. Tables with basic parameters, time-series *I*- and *V*-band photometry, and finding charts are available to the astronomical community through the OGLE On-line Data Archive:

<http://ogle.astrouw.edu.pl>

and <ftp://ftp.astrouw.edu.pl/ogle/ogle4/OCVS/blg/dsct/>

The stars are arranged according to increasing right ascension and named as OGLE-BLG-DSCT-NNNNN, where NNNNN is a five-digit consecutive number. In the data tables, we provide coordinates of the variables, the dominant pulsation period, period uncertainty, and information on brightness.

Among the 10 111 detected  $\delta$  Sct variables only two stars have a GCVS designation (Samus *et al.* 2017). Variables OGLE-BLG-DSCT-06456 = V1363 Sgr

and OGLE-BLG-DSCT-06718 = V4117 Sgr were discovered by Blanco (1984) and Gaposchkin (1955), respectively. The latter object is located in the field of globular cluster NGC 6522 (variable V6, Clement *et al.* 2001) in Baade's Window area, but the star probably does not belong to the cluster. Other 42  $\delta$  Sct stars were identified in OGLE-I data (Udalski *et al.* 1994, 1995ab, 1996, 1997). Seventy-six of the variables were found by the MACHO team (Alcock *et al.* 2000). Another 139 sources were later recognized in OGLE-II data by Pigulski *et al.* (2006). Seven  $\delta$  Sct pulsators were recently detected by the ASAS-SN survey (Jayasinghe *et al.* 2020). Ten additional objects were found in the field of globular clusters M22 (seven stars, Kaluzny and Thompson 2001, Rozyczka *et al.* 2017) and M54 (three stars, Sollima *et al.* 2010), and classified as SX Phe stars. In total, 276 variables from our collection were known before, or 9835 OGLE-IV  $\delta$  Sct variables are new discoveries. Other designations are also provided in the on-line data.

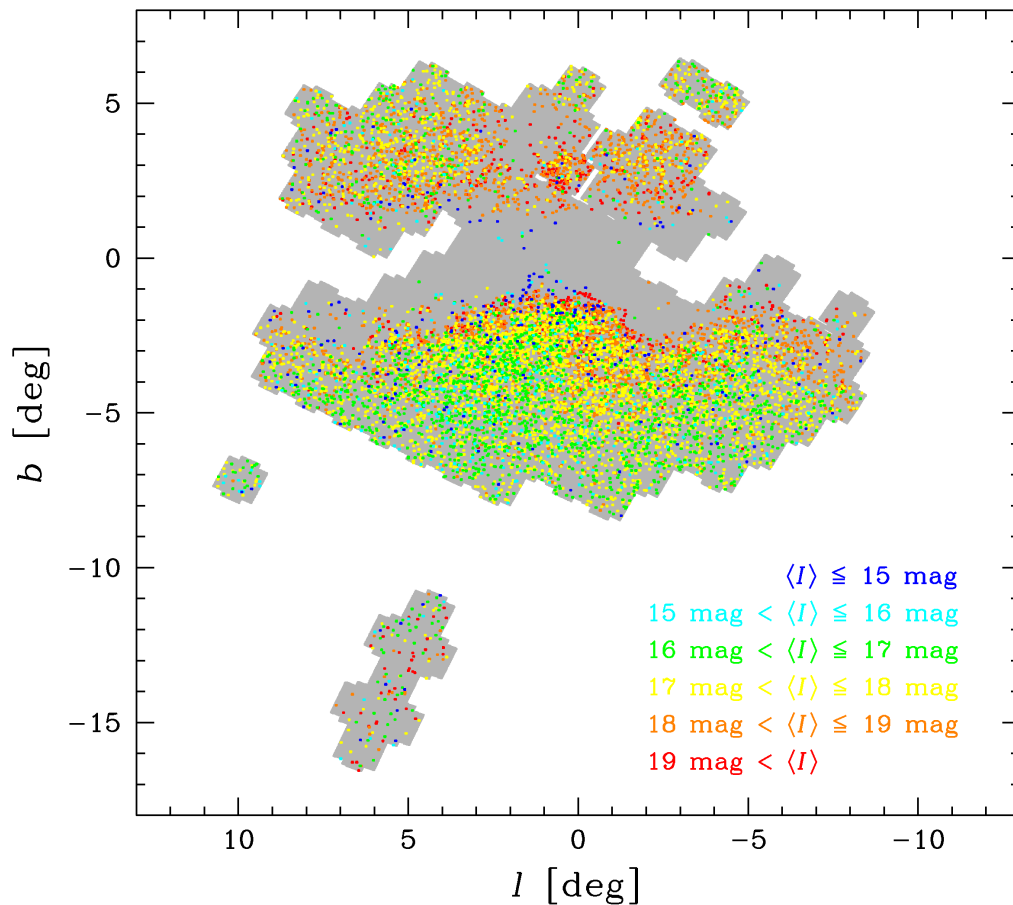


Fig. 1. Distribution in Galactic coordinates of 10 111  $\delta$  Sct-type variable stars detected in 121 OGLE-IV bulge fields (marked in grey) spreading over  $172 \text{ deg}^2$ . Seven fields located around  $(l, b) = (+5^\circ, -13^\circ)$  cover the central part of the Sgr dSph galaxy. A single outlying field at  $(l, b) \approx (+10^\circ, -7^\circ)$  includes Galactic globular cluster M22. The colors code mean  $I$ -band brightness of the variables.

#### 4. General Properties of the Detected $\delta$ Sct Stars

The new collection is a source of various information on the  $\delta$  Sct stars themselves and stellar populations they belong to. In this section, we present some general properties of the detected stars.

Fig. 1 shows the distribution of the  $\delta$  Sct variables overlaid onto the contours of the 121 investigated OGLE-IV Galactic bulge fields. Due to the increasing interstellar extinction toward the Galactic plane, the variables get fainter and they are practically not observed at low latitudes ( $|b| < 1^\circ$ ) in the optical range. The stars concentrate toward the Galactic center. This suggests that most of the detected  $\delta$  Sct objects are located at distances of several kpc or more from us and that they mainly belong to the intermediate-age and old populations. Some of the stars are likely metal-poor representatives of the old disk and halo components and could be classified as SX Phe-type variables. Nevertheless, most of the variables seem to belong to the Galactic bulge.

For variables with available  $V$ -band data it was possible to construct an observed color–magnitude diagram presented in Fig. 2. The majority of  $\delta$  Sct stars are smeared in a lane parallel to the reddening vector (determined from the OGLE bulge RR Lyr stars, Pietrukowicz *et al.* 2015). Stars above the lane (brighter) are foreground, likely halo and thick disk objects. Stars below the lane (fainter) form-

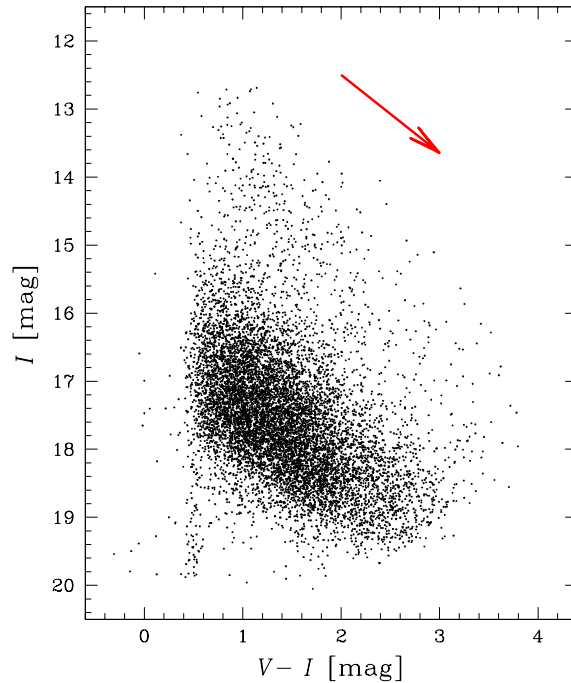


Fig. 2.  $(V - I)$  vs.  $I$  diagram for 9579  $\delta$  Sct stars. The arrow represents the reddening vector in the bulge area. Points forming a sequence around the color  $V - I = 0.5$  mag in the brightness range  $18 < I < 20$  mag are background  $\delta$  Sct stars from the Sgr dSph galaxy.

ing a vertical sequence at  $V - I \approx 0.5$  mag, belong to the Sgr dSph galaxy which core, the globular cluster M54, is located at the distance of 26.7 kpc (*e.g.*, Hamanowicz *et al.* 2016). It is worth noting that the on-sky distribution and the color–magnitude diagram for  $\delta$  Sct stars are very similar to those of bulge RR Lyr variables (see Fig. 2 in Soszyński *et al.* 2014 and Fig. 1 in Pietrukowicz *et al.* 2015, respectively).

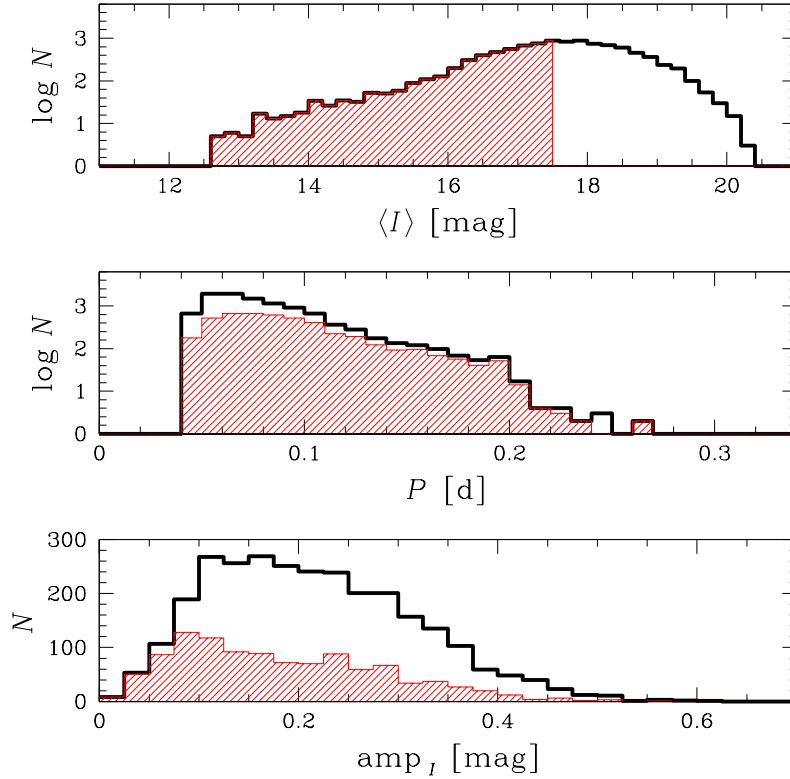


Fig. 3. *Upper panel*: Mean  $I$ -band brightness distribution for the whole set of 10 111 OGLE-IV  $\delta$  Sct variables. The bin size is 0.2 mag. The vertical axis has a logarithmic scale. High completeness of the sample reaches a magnitude of  $I = 17.5$  (shaded in red). *Middle panel*: Histogram of the dominant period for all detected 10 111  $\delta$  Sct stars (black line) and 4533 variables brighter than  $\langle I \rangle = 17.5$  mag (in red). The bin size is 0.01 d. The vertical axis has a logarithmic scale. *Lower panel*: Histogram of the peak-to-peak  $I$ -band amplitude determined for all 2880 single-mode  $\delta$  Sct pulsators (black line) and 1075 single-mode pulsators with  $\langle I \rangle < 17.5$  mag (shaded in red). The bin size is 0.025 mag.

Fig. 3 contains three panels with, from top to bottom, the mean  $I$ -band brightness, pulsation period, and peak-to-peak  $I$ -band amplitude distributions of detected  $\delta$  Sct stars. The amplitudes were determined for 2880 single-mode pulsators only. Based on the brightness and amplitude distributions we can infer that the presented collection is highly complete for variables with the mean  $I$ -band brightness  $< 17.5$  mag and with amplitudes higher than 0.1 mag. The maximum of the pe-

riod distribution is at about 0.07 d for the brighter variables ( $I \leq 17.5$  mag).<sup>‡</sup> It is impossible to separate shorter-period metal-poor Population II (SX Phe) stars from longer-period metal-rich Population I  $\delta$  Sct stars by the pulsation period. The former pulsators are likely much less abundant in the whole sample.

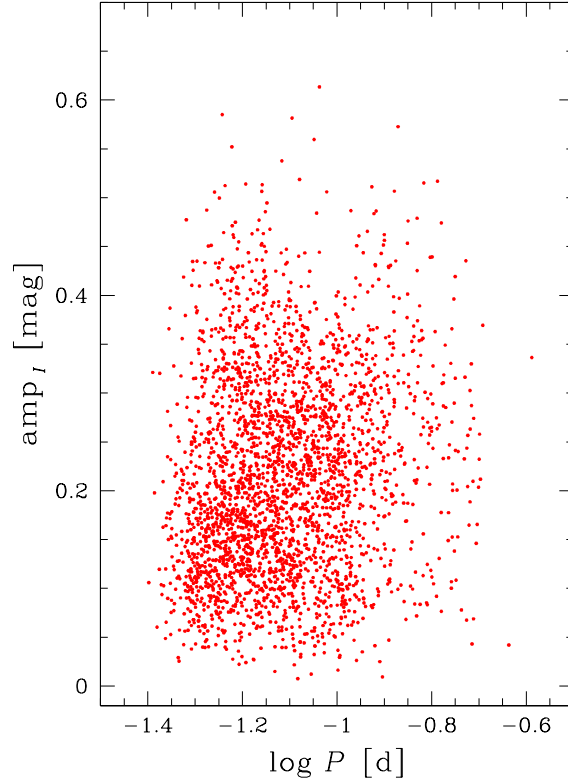


Fig. 4. Period–amplitude diagram for 2880 single-mode  $\delta$  Sct stars. There are no evident features in this diagram.

Period–amplitude diagram is shown in Fig. 4. There are no characteristic features in this diagram, in contrast to such (Bailey) diagram for RR Lyr stars (Soszyński *et al.* 2014).

We decomposed the light curves of single-mode pulsators into cosine Fourier series. In Fig. 5, we plot the Fourier coefficient combinations, amplitude ratio  $R_{21}$  and  $R_{31}$ , and phase combinations  $\phi_{21}$  and  $\phi_{31}$ , in the function of period. The phase combinations clearly correlate with the period.

<sup>‡</sup>In the whole collection, there is only one variable with a pulsation period below 0.04 d (OGLE-BLG-DSC1-09299 with  $P_{\text{puls}} = 0.0399$  d) and thus it is not seen in the logarithmic scale histogram in Fig. 3. Many inspected variable sources with periods below 0.04 d and not classified by us as BLAPs have sinusoidal or nearly sinusoidal light curve shapes. Those objects could be SX Phe variables as well as pulsating variables of other types (*e.g.*, subdwarfs, white dwarfs). We plan to analyze the shortest-period objects separately.

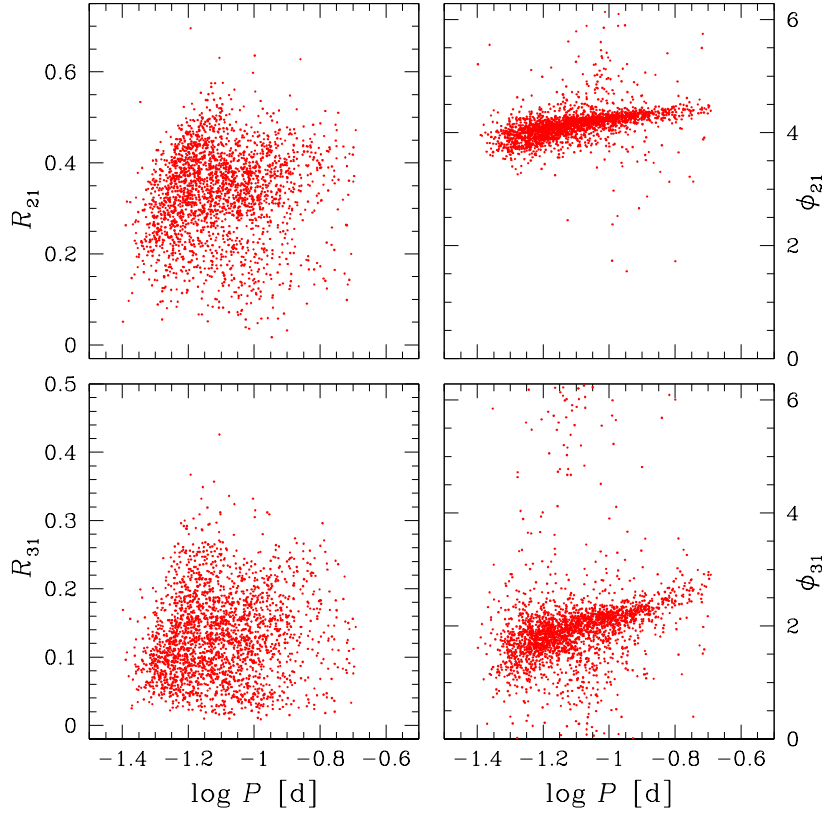


Fig. 5. Fourier coefficient combinations  $R_{21}$ ,  $R_{31}$ ,  $\phi_{21}$ , and  $\phi_{31}$  as a function of the logarithm of the pulsation period for single-mode  $\delta$  Sct stars. Evident correlations are seen for both Fourier phase combinations.

## 5. Possible Members of Globular Clusters

Some of the variables in this collection belong or likely belong to globular clusters. We scanned the whole sample for  $\delta$  Sct/SX Phe stars in the area of 37 globular clusters observed in the OGLE-IV bulge fields. In Table 1, we present a list of 22 variables located within three half-light radii ( $r < 3r_h$ ) from the centers of nine clusters. We used a brightness criterion that SX Phe stars are about 1.7–3.3 mag fainter in  $V$  than the horizontal branch (HB) of the cluster (*e.g.*, Kaluzny *et al.* 1996, Kaluzny and Thompson 2001). Parameters of the clusters (coordinates, radii, HB magnitudes) were taken from Harris (1996) catalog (version 2010). Seven objects in globular cluster M22 (NGC 6656) were previously known (Kaluzny and Thompson 2001, Rozyczka *et al.* 2017) and are confirmed members (Zloczewski *et al.* 2012, Rozyczka *et al.* 2017). The remaining 15 variables could belong to the clusters. We performed a similar scanning operation for the radius  $r < 5r_h$  finding 35 objects. However, one has to remember that most of the observed clusters are immersed in relatively dense bulge environment and separating bulge from cluster stars can be problematic at larger distances from the cluster centers.

Table 1

OGLE-IV  $\delta$  Sct/SX Phe variables located within the radius of  $3r_h$  from the centers of globular clusters

Cluster	Variable OGLE-BLG- -DSCT-	$\langle I \rangle$ [mag]	$\langle V \rangle$ [mag]	$P_{\text{puls}}$ [d]	$r/r_h$	Other name
NGC 6304	00038	17.00	17.95	0.08804739(1)	2.30	
	00055	17.63	18.64	0.08810378(2)	1.71	
	00057	17.77	18.78	0.06559091(1)	2.45	
NGC 6401	01179	18.57	20.28	0.05328611(1)	2.80	
	01209	18.22	19.73	0.10545024(4)	1.26	
	01243	18.77	20.18	0.06473004(1)	2.46	
Pal 6	01905	18.68	21.37	0.10669881(4)	1.86	
NGC 6453	03154	18.57	19.72	0.05319618(1)	2.03	
Djorg 2	06270	18.27	19.88	0.04707594(1)	2.50	
NGC 6544	07604	15.68	17.10	0.08068763(1)	0.48	
	07630	16.03	17.46	0.04352380(1)	0.95	
NGC 6558	08161	17.35	18.25	0.05704527(1)	2.47	
	08283	17.13	18.02	0.05511362(2)	2.36	
NGC 6569	08825	18.58	19.51	0.05483726(4)	1.00	
M22	09961	15.98	16.81	0.04731774(4)	0.59	KT-34 <sup>1</sup>
	09963	15.66	16.42	0.04432495(2)	0.50	KT-29 <sup>1</sup>
	09964	15.31	16.17	0.05560342(7)	0.66	KT-28 <sup>1</sup>
	09965	15.81	16.63	0.05007784(2)	0.18	KT-45 <sup>1</sup>
	09966	16.08	16.89	0.04217440(3)	0.29	KT-27 <sup>1</sup>
	09967	15.54	16.33	0.08364628(3)	1.03	KT-54 <sup>1</sup>
	09968	14.86	15.94	0.06231611(2)	0.12	V112 <sup>2</sup>
	09969	15.68	16.44	0.1077372(2)	1.39	

Mean brightness, pulsation period, and distance from the cluster center are provided for each variable. Seven members of globular cluster M22 were previously reported in <sup>1</sup>Kaluzny and Thompson (2001), and <sup>2</sup>Rozyczka *et al.* (2017).

## 6. Peculiarities in the $\delta$ Sct Light Curves

In this section, we illustrate the variety of light curve shapes of the  $\delta$  Sct pulsators. Some of the presented objects resemble variables of other types. Very often, the shape, period, and peak-to-peak amplitude allow unambiguous classification. In some cases, however, to confirm that the variables are indeed of the  $\delta$  Sct type, we additionally verified their positions in color–magnitude diagrams constructed for stars from the same field. The  $\delta$  Sct stars reside in the area around the upper or middle MS in the observed diagrams.

In Fig. 6, we show four examples of high-amplitude  $\delta$  Sct stars with nearly flat minima. The minima cover up to about 0.4 of the cycle. High amplitudes and sharp

maxima point to the fundamental mode. Variables with such light curve shape have periods in the range roughly 0.05–0.07 d.

Fig. 7 presents four  $\delta$  Sct variables with sharp maxima and almost symmetric shape. Such shape resembles light curves of binary systems with a prominent reflection effect due to large difference in effective temperature between the components (for instance, in hot subdwarf–brown dwarf binaries). The mild asymmetry at the period of a few hours clearly indicates that these objects are pulsating  $\delta$  Sct stars. The round minima and low amplitudes of  $\approx 0.1$  mag point to an overtone mode.

In Fig. 8, we present another group of nearly symmetric light curves of  $\delta$  Sct variables. This group mimics contact binary systems if double the period. Nevertheless, even the doubled period is shorter than the orbital period observed in almost all contact binaries ( $> 0.2$  d). *I*-band amplitudes of such  $\delta$  Sct variables are of about 0.1 mag or smaller.

In the following figure, Fig. 9, one can find  $\delta$  Sct variables showing reverse brightness variation to typical pulsating stars – the time from the minimum to the maximum is longer than the time from the maximum to the minimum. An identical shape, with a broken rising branch half-way to the maximum light, was already found in a triple-mode classical Cepheid OGLE-SMC-CEP-1350 (see Fig. 5 in Soszyński *et al.* 2010). Light curve decomposition of that star pointed to the first overtone. By analogy, we suspect that the bulge objects presented in Fig. 9 are first-overtone pulsators.

In Fig. 10, we present examples of  $\delta$  Sct light curves with sharp extrema. Fig. 11 shows variables with pronounced additional bumps on both the rising and fading branches. Such light curve shapes are observed in the period range from about 0.07 d to 0.09 d.

In Fig. 12, we compare phased, saw-tooth-shaped light curves of presumably fundamental-mode  $\delta$  Sct pulsators in a wide period range of 0.05–0.2 d. Amplitudes of the stars were not scaled. One can follow the evolution of the light curve shape with the increasing period similar to the Hertzsprung progression in Cepheids. The light curve of a 0.05-d fundamental-mode  $\delta$  Sct star is very similar in shape to a 1.0-d classical Cepheid and 0.9-d anomalous Cepheid showing a small bump around the minimum light. The shape of a 0.2-d  $\delta$  Sct star resembles the shape of a 5-d classical Cepheids with the bump appearing on the fading branch.

During the visual inspection of  $\delta$  Sct light curves, we encountered many evident multi-mode pulsators. Detailed analysis of additional periodicities is presented in Netzel *et al.* (in preparation). Here in Fig. 13, we show three double-mode  $\delta$  Sct stars pulsating in the fundamental mode (F) and first overtone (1O), simultaneously. The mode types are confirmed by relatively high amplitudes of 0.1–0.2 mag and the period ratio  $P_{1O}/P_F \approx 0.77$  (see sequences in the Petersen diagram in Fig. 10 in Pietrukowicz *et al.* 2013). In the power spectrum, the presented stars also show a combination frequency  $f = f_{1O} - f_F$ , which proves the intrinsic origin

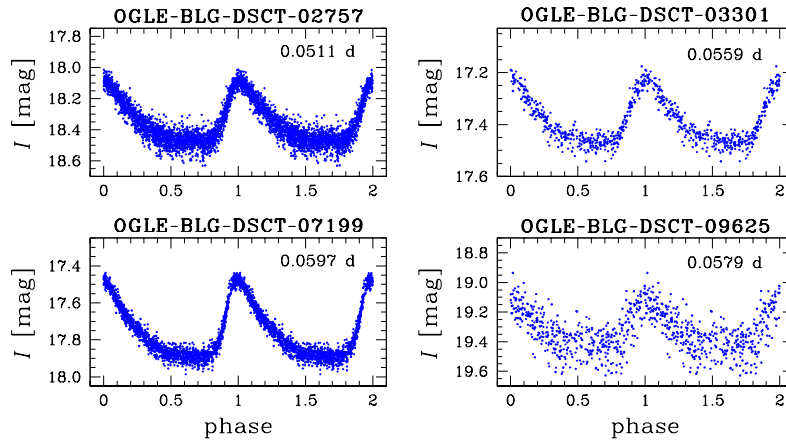


Fig. 6. Phased *I*-band light curves of selected  $\delta$  Sct variables with wide, nearly flat minima.

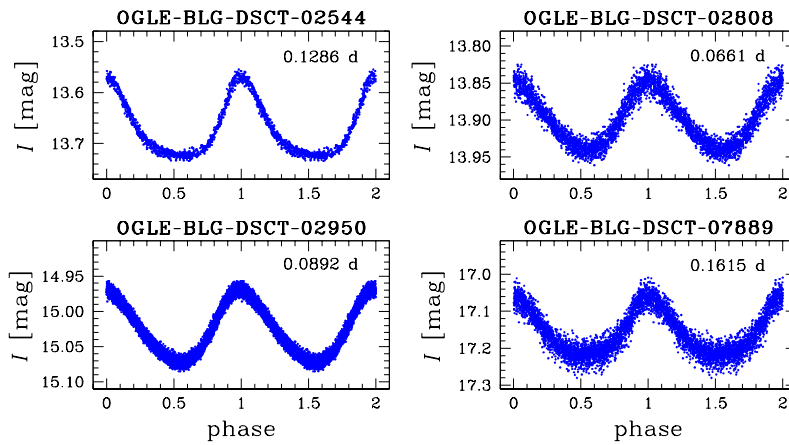


Fig. 7. Examples of  $\delta$  Sct variables with nearly symmetric light curves.

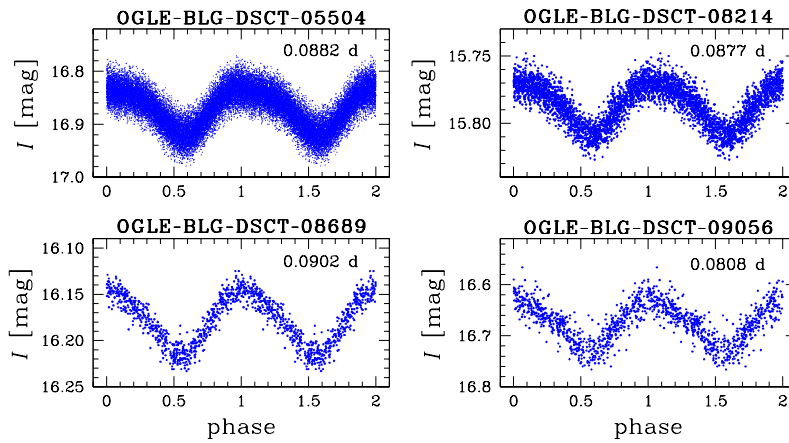


Fig. 8. Examples of  $\delta$  Sct variables that mimic contact binary stars when double the given period.

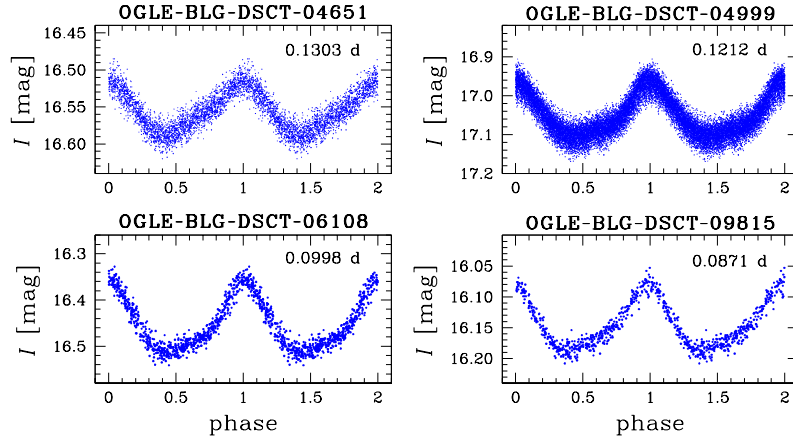


Fig. 9. Examples of phased light curves of  $\delta$  Sct variables with the rising part lasting longer than the fading one. These are likely first overtone pulsators.

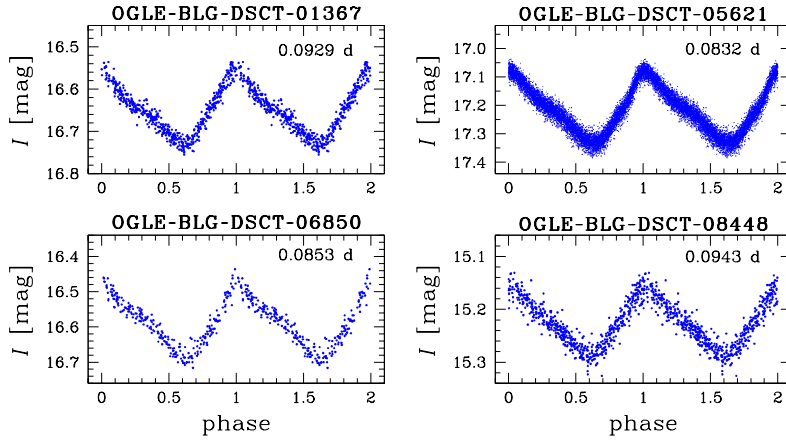


Fig. 10. Light curves of  $\delta$  Sct variables with sharp extrema.

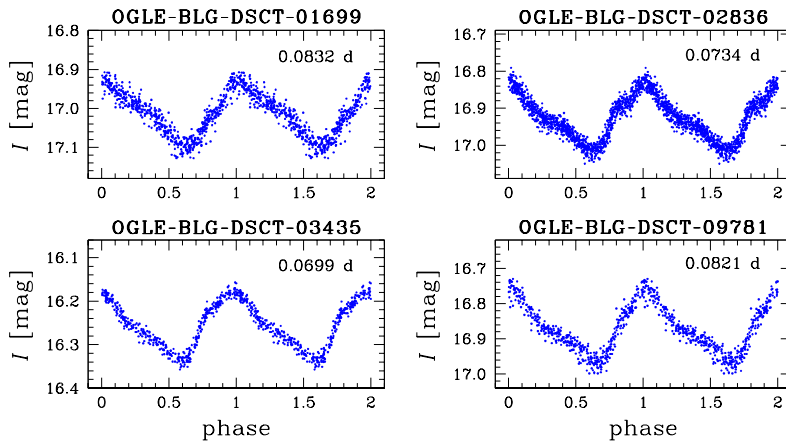


Fig. 11.  $\delta$  Sct variables with bumps on the rising and fading branches.

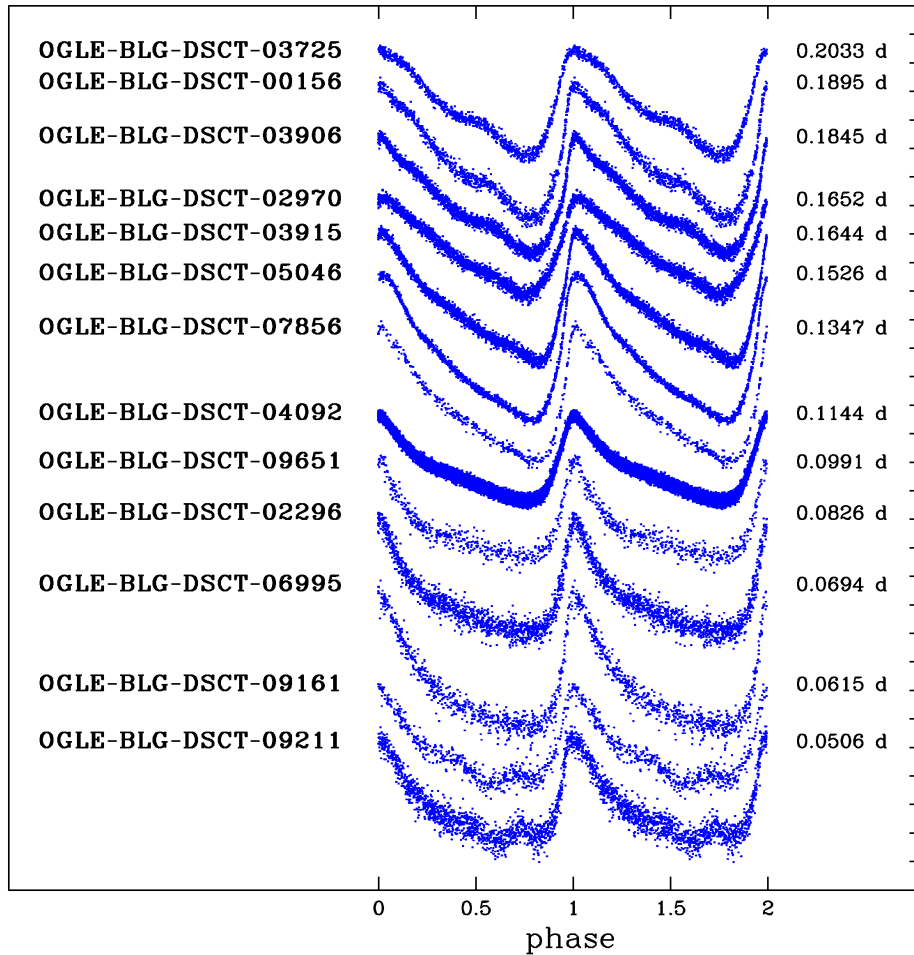


Fig. 12. Light curve shape changes with the pulsation period in fundamental-mode  $\delta$  Sct stars. The light curves are shifted to avoid overlaps, but the amplitudes are preserved. The ticks on the vertical axis are every 0.1 mag.

of the double-mode signal. We would like to pay attention to the shape of the first-overtone component in star OGLE-BLG-DSCT-00875. Light curves of a similar shape with round symmetric minima, are observed in some other  $\delta$  Sct stars (see Fig. 14). In these stars, the dominant mode seems to be the first overtone.

In Fig. 15, we show a few examples of  $\delta$  Sct stars with mean brightness variations observed over the whole decade of OGLE-IV. In object OGLE-BLG-DSCT-05430, for instance, the mean  $I$ -band brightness dropped monotonically by 0.15 mag. In star OGLE-BLG-DSCT-07133, the mean brightness varied irregularly over the years 2010–2019 reaching an amplitude of 0.053 mag. The observed variations may stem from the presence of an active companion to the pulsating star.

Some of the  $\delta$  Sct stars exhibit noticeable period changes. Fig. 16 contains four such examples. In each panel, we overplot the phased light curve from 2014 onto

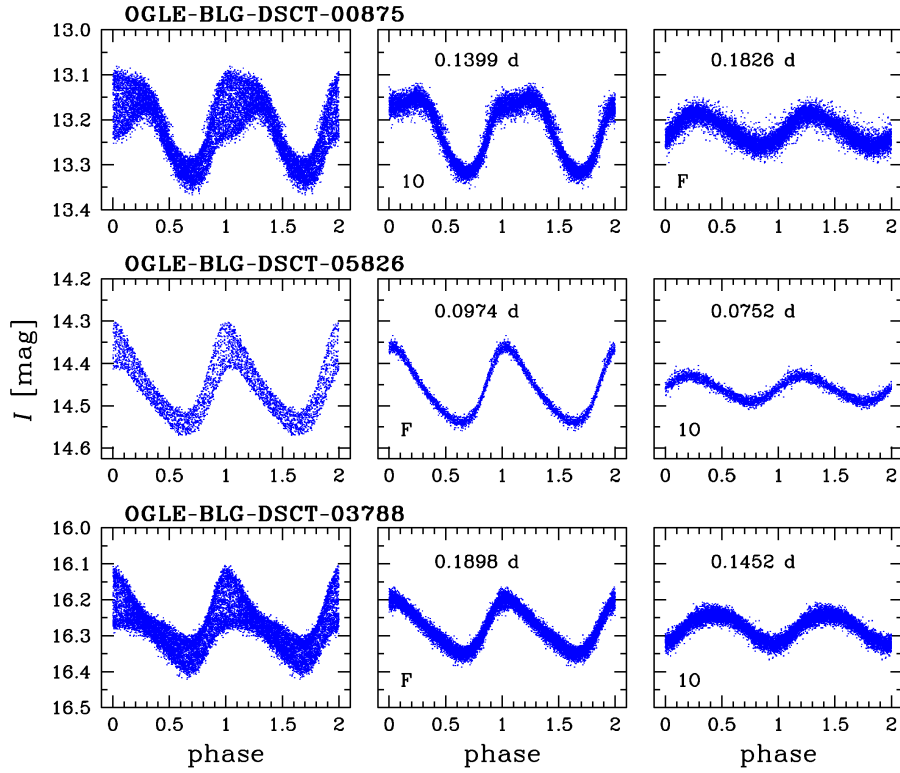


Fig. 13. Three examples of double-mode (fundamental + first overtone)  $\delta$  Sct pulsators. Note an unusual shape of the first overtone component in star OGLE-BLG-DSCT-00875 (*top middle panel*).

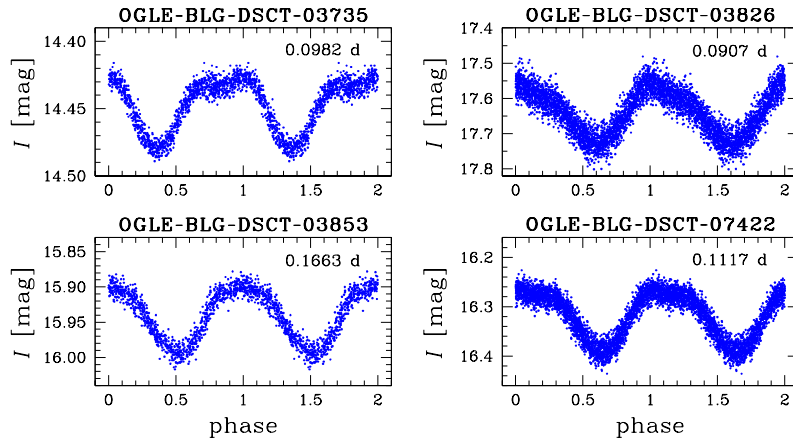


Fig. 14. Four examples of first-overtone  $\delta$  Sct pulsators showing the unusual shape encountered in OGLE-BLG-DSCT-00875 (see Fig. 13).

the full OGLE-IV light curve. In the case of object OGLE-BLG-DSCT-06232, the changes seem to be large. A detailed analysis of period changes in  $\delta$  Sct stars is planned in a separate article.

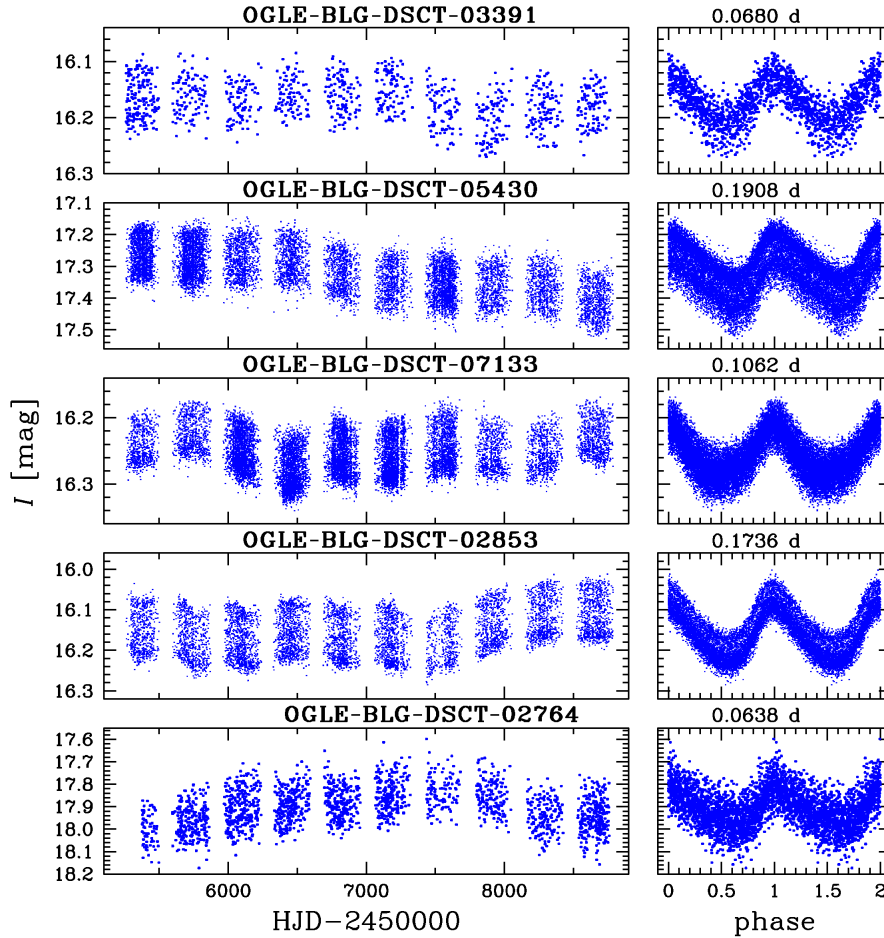


Fig. 15. Examples of  $\delta$  Sct variables showing mean brightness variations over the years 2010–2019.

We found dozens of  $\delta$  Sct stars with amplitude changes. Five most prominent examples are presented in Fig. 17. In each case, we selected two seasons for comparison of the phased light curves. In some stars, such as OGLE-BLG-DSCT-01200, the amplitude variations may have a cyclic behavior.

The correction of the period values applied to the data covering the whole observing decade led us to the discovery of six  $\delta$  Sct stars in which the pulsation signal greatly weakened or even disappeared. Time-domain light curves of the stars and power spectra for two selected periods of time are shown in Fig. 18. Pulsations could stop at all in stars OGLE-BLG-DSCT-00672, OGLE-BLG-DSCT-02036, OGLE-BLG-DSCT-07325, OGLE-BLG-DSCT-08138. However, a more likely explanation is that, for a period of time (months to years), the pulsations may have had too low amplitude to be detected in ground-based data. In objects OGLE-BLG-DSCT-05035 and OGLE-BLG-DSCT-05668, the dominant pulsation frequencies are seen in the power spectra all the time but with changing strength.

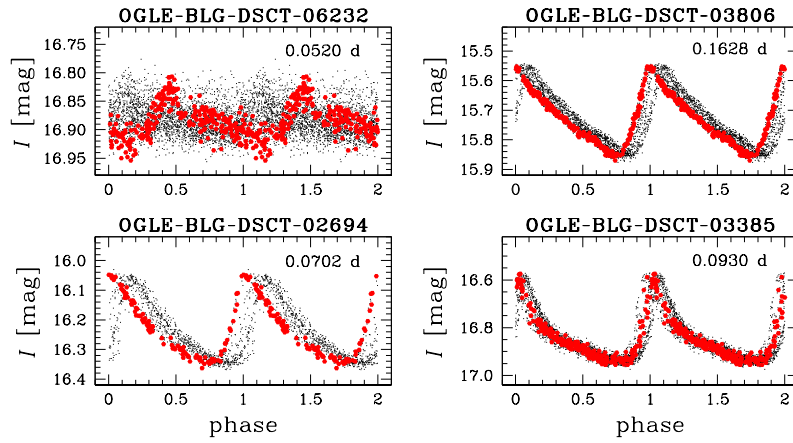


Fig. 16. Selected  $\delta$  Sct stars with evident period changes. Red points are measurements from 2014 against decade-long data in black.

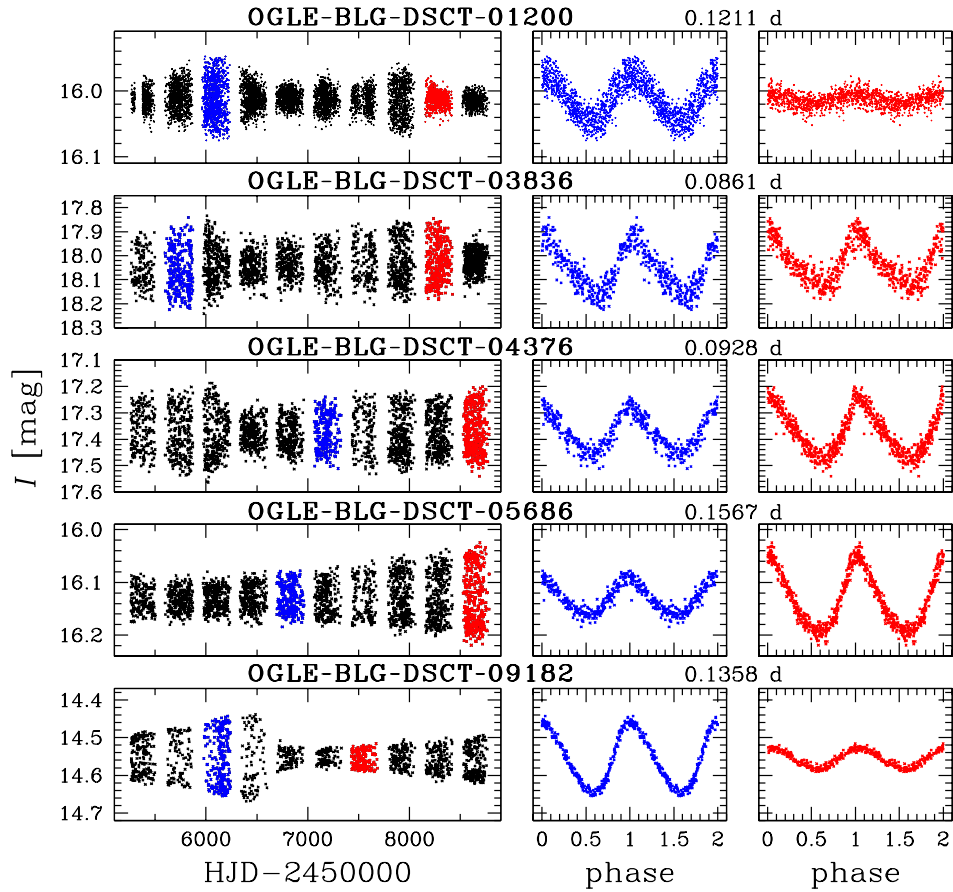


Fig. 17. Examples of  $\delta$  Sct variables with large amplitude changes. *Left column*: time-domain data. *Middle and right columns*: phased light curves from two selected seasons (marked in blue and red in the time-domain curve). The magnitude range on the vertical axis is the same for each row.

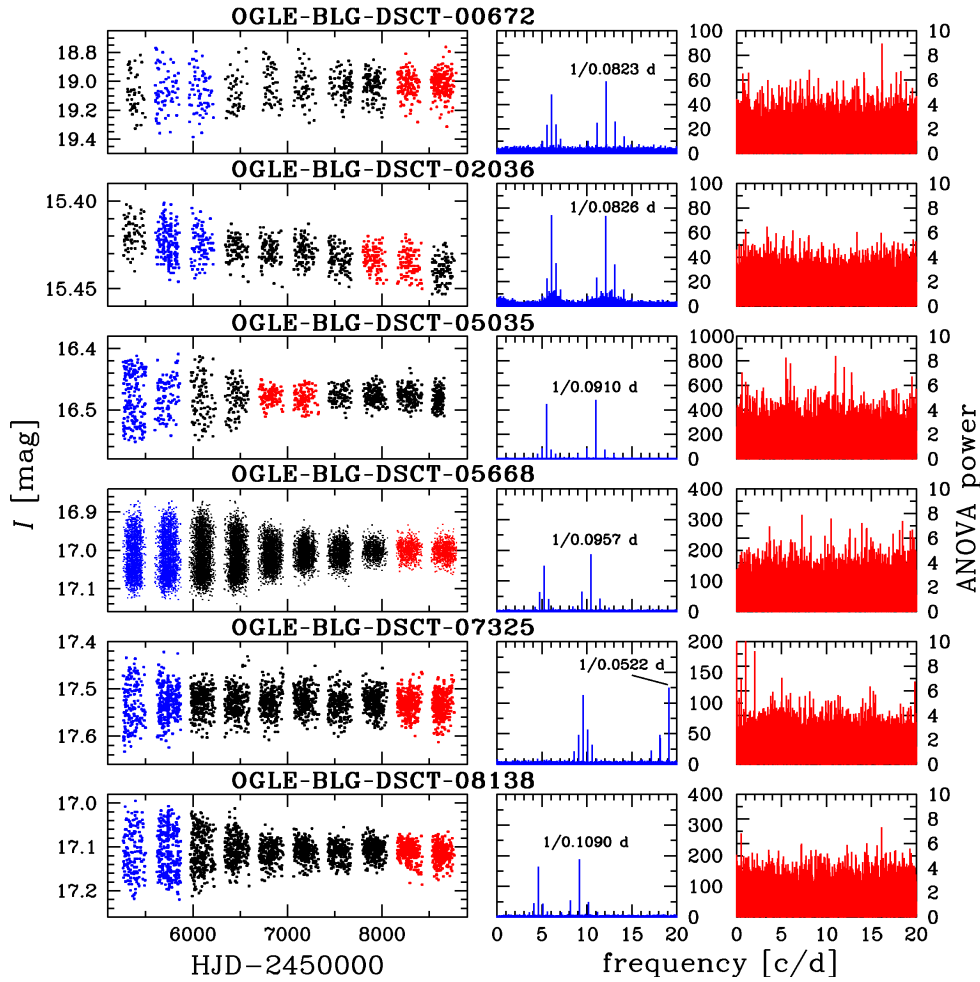


Fig. 18.  $\delta$  Sct variables with significant attenuation or complete lack of the pulsation signal over a period of time. *Left column*: time-domain data. *Middle column*: power spectra from observational seasons with strong pulsation signal (marked in blue). *Right column*: power spectra from seasons with weak or vanished pulsation signal (marked in red). The power range in quiescence is magnified.

In the former object, the signal was strong in years 2010–2011, very weak in years 2014–2015, and then it became stronger again, as the amplitude increased.

The visual inspection of original light curves of all  $\delta$  Sct variables and light curves of multi-periodic variables after prewhitening for the dominant period allowed us to find fourteen sources with additional eclipsing or ellipsoidal binary variations. Table 2 lists parameters of the sources. Three of the variables were already classified as binary stars in Soszyński *et al.* (2016). In Fig. 19, we decompose the signal into the pulsation and orbital components for four selected objects. In some of the sources, in particular those with short-period orbital variations, the light from the  $\delta$  Sct star can be blended with the binary signal from other object in the line of sight. Follow-up spectroscopic observations would confirm whether the listed  $\delta$  Sct stars form physical systems.

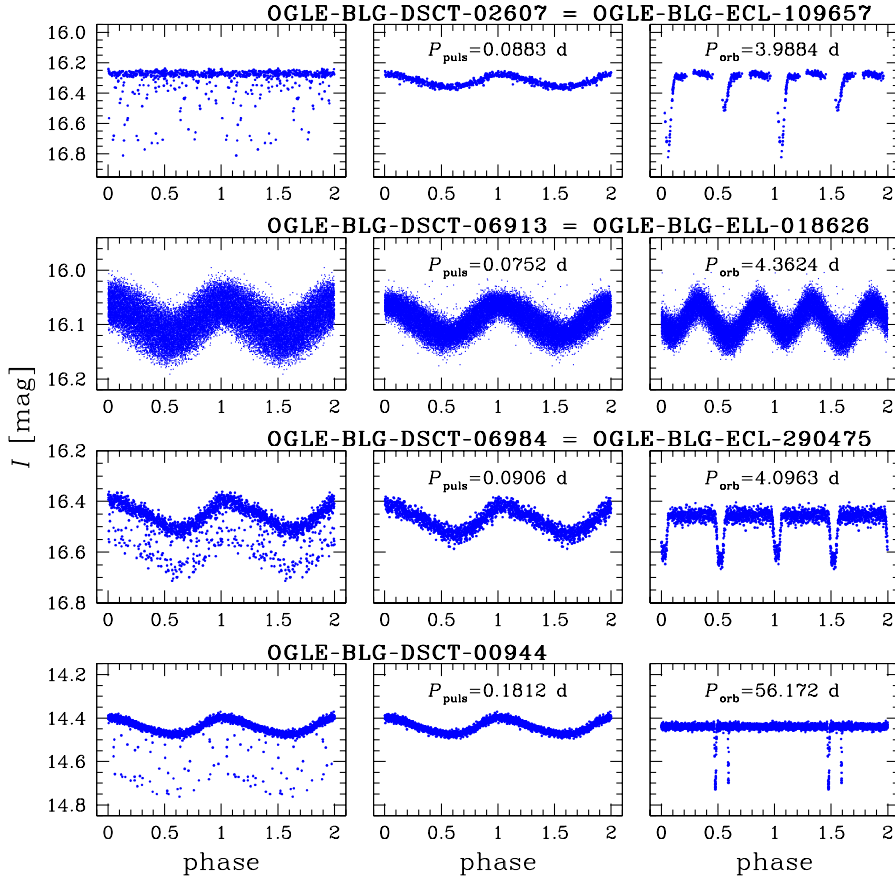


Fig. 19. Four  $\delta$  Sct pulsators with additional binary modulation. *Left column*: original light curves folded with the pulsation period. *Middle and right columns*: pulsation and binary components folded with the pulsation and orbital periods, respectively. Top three variables were already classified as binary systems in Soszyński *et al.* (2016).

## 7. Summary

Our search for short-period objects in the OGLE-IV photometric data covering  $172 \text{ deg}^2$  of the Galactic bulge and spanning the decade 2010–2019 brought the identification of 10 111 genuine  $\delta$  Sct-type variable stars. About 97.3% of the sample (exactly 9835 stars) are newly discovered variables. Most of the stars (71.5%) are multi-mode pulsators. We showed graphically a huge variety of light curve shapes of  $\delta$  Sct stars, a much greater diverse than observed in other classical pulsators (*i.e.*, Cepheids and RR Lyr stars). The shapes, periods, and amplitudes in  $\delta$  Sct stars vary greatly. We found six stars in which the pulsation signal had vanished. In one case, it reappeared. Most likely, the signal was, or in some stars still is, too faint to be detected in ground-based photometry, obtained even from a superb astronomical site such as the Las Campanas Observatory, Chile. There is additional eclipsing or ellipsoidal modulation in fourteen  $\delta$  Sct stars. Spectroscopic follow-up

Table 2  
 $\delta$  Sct variables with additional eclipsing or ellipsoidal modulation

Variable OGLE-BLG- -DSCT-	$\langle I \rangle$ [mag]	$\langle V \rangle$ [mag]	$P_{\text{puls}}$ [d]	Binarity type	$P_{\text{orb}}$ [d]
00944	14.40	16.86	0.18121235(5)	EA	56.172(1)
02533	15.67	17.23	0.08915221(4)	EA	7.1610(3)
02607	16.31	17.46	0.08832817(4)	EB	3.98843(4)
03141	17.90	20.61	0.15680356(8)	EW	0.3390154(2)
04442	16.79	17.92	0.07464503(3)	EW	4.20527(3)
04527	17.44	19.56	0.06478072(4)	EW	3.674495(19)
04548	16.90	18.16	0.07158575(1)	EW	3.15517(5)
05241	17.99	19.58	0.07006432(4)	EW	0.27519460(12)
05566	18.05	–	0.06349199(1)	EW	0.2655016(2)
06021	16.78	17.87	0.08031543(4)	Ell	5.10522(7)
06913	16.09	17.33	0.07524575(5)	Ell	4.362363(12)
06984	16.48	–	0.09059884(5)	EA	4.096252(9)
07078	17.51	18.77	0.04974273(1)	EA	1.205674(2)
07460	17.30	18.26	0.04894781(1)	EW	0.4543568(2)

Mean brightness, pulsation period, detected binarity type, and orbital period are provided for each variable.

observations would confirm whether the pulsators possess physically bound companions which would allow accurate determination of binary system parameters.

Our sample includes SX Phe-type stars, but it is impossible to distinguish between the Population II stars and Population I stars based on the OGLE photometry only. The two groups cannot be separated by the pulsation period what we hoped for before.

The presented collection of  $\delta$  Sct stars has many potential applications to various areas of stellar astrophysics, such as asteroseismology, galactic population studies, and distance scale determination.

**Acknowledgements.** We thank OGLE observers for their contribution to the collection of the photometric data over the years. The OGLE project has received funding from the National Science Centre, Poland, through grant number MAESTRO 2014/14/A/ST9/00121 to AU. This work has also been supported by the National Science Centre, Poland, grants OPUS 2016/23/B/ST9/00655 to PP and MAESTRO 2016/22/A/ST9/00009 to IS. HN acknowledges support from the Polish Ministry of Science and Higher Education under grant 0192/DIA/2016/45 within the Diamond Grant Programme for years 2016-2021 and Foundation for Polish Science (FNP).

## REFERENCES

- Alard, C., and Lupton, R.H. 1998, *ApJ*, **503**, 325.
- Alcock, C., *et al.* 2000, *ApJ*, **536**, 798.
- Balona, L.A., and Dziembowski, W.A. 2011, *MNRAS*, **417**, 591.
- Bellm, E.C., *et al.* 2019, *PASP*, **131**, 018002.
- Blanco, B. M. 1984, *AJ*, **89**, 1836.
- Breger, M., *et al.* 2000, *ASP Conf. Ser.*, **210**, 3.
- Campbell, W.W., and Wright, W.H. 1900, *ApJ*, **12**, 254.
- Chang, S.-W., Protopapas, P., Kim, D.-W., and Byun, Y.-I. 2013, *AJ*, **145**, 132.
- Chen, X., Wang, S., Deng, L., de Grijs, R., Yang, M., and Tian, Hao 2020, *ApJS*, **249**, 18.
- Clement, C.M., *et al.* 2001, *AJ*, **122**, 2587.
- Colacevich, A. 1935, *PASP*, **47**, 231.
- Eggen, O.J. 1956a, *PASP*, **68**, 238.
- Eggen, O.J. 1956b, *PASP*, **68**, 541.
- Fath, E.A. 1935, *PASP*, **47**, 232.
- Fath, E.A. 1937, *Lick Obs. Bull.*, **18**, 77.
- Gaposchkin, S.I. 1955, *Per. Zvez.*, **10**, 337.
- Hamanowicz, A., *et al.* 2016, *Acta Astron.*, **66**, 197.
- Harris, W.E. 1996, *AJ*, **112**, 1487.
- Jayasinghe, T., *et al.* 2020, *MNRAS*, **493**, 4186.
- Kaluzny, J., Kubiak, M., Szymański, M., Udalski, A., Krzeminski, W., and Mateo, M. 1996, *A&AS*, **120**, 139.
- Kaluzny, J., and Thompson, I.B. 2001, *A&A*, **373**, 899.
- Kochanek, C.S., *et al.* 2017, *PASP*, **129**, 104502.
- Lindblad, P.O., and Eggen, O.J. 1953, *PASP*, **65**, 291.
- Mazur, B., Krzemiński, W., and Thompson, I.B. 2003, *MNRAS*, **340**, 1205.
- McNamara, D.H. 2011, *AJ*, **142**, 110.
- Murphy, S.J., Hey, D., Van Reeth, T., and Bedding, T.R. 2019, *MNRAS*, **485**, 2380.
- Pietrukowicz, P., *et al.* 2013, *Acta Astron.*, **63**, 379.
- Pietrukowicz, P., *et al.* 2015, *ApJ*, **811**, 113.
- Pietrukowicz, P., *et al.* 2017, *Nature Astronomy*, **1**, 166.
- Pigulski, A., Kołaczowski, Z., Ramza, T., and Narwid, A. 2006, *Memorie della Società Astron. Italiana*, **77**, 223.
- Pojmański, G. 2002, *Acta Astron.*, **52**, 397.
- Poleski, R., *et al.* 2010, *Acta Astron.*, **60**, 1.
- Pych, W., Kaluzny, J., Krzeminski, W., Schwarzenberg-Czerny, A., and Thompson, I.B. 2001, *A&A*, **367**, 148.
- Rodríguez, E., López-González, M.J., and López de Coca, P. 2000, *A&AS*, **144**, 469.
- Rodríguez, E., and López-González, M.J. 2000, *A&A*, **359**, 597.
- Rozyczka, M., Thompson, I.B., Pych, W., Narloch, W., Poleski, R., and Schwarzenberg-Czerny, A. 2017, *Acta Astron.*, **67**, 203.
- Samus, N.N., Kazarovets, E.V., Durlevich, O.V., Kireeva, N.N., and Pastukhova, E.N. 2017, *Astronomy Reports*, **61**, 80.
- Schwarzenberg-Czerny, A. 1996, *ApJ*, **460**, L107.
- Shappee, B.J., *et al.* 2014, *ApJ*, **788**, 48.
- Sollima, A., Cacciari, C., Bellazzini, M., and Colucci, S. 2010, *MNRAS*, **406**, 329.
- Soszyński, I., *et al.* 2010, *Acta Astron.*, **60**, 17.
- Soszyński, I., *et al.* 2014, *Acta Astron.*, **64**, 177.
- Soszyński, I., *et al.* 2016, *Acta Astron.*, **66**, 405.
- Sterne, T.E. 1938, *ApJ*, **87**, 133.
- Templeton, M.R., McNamara, B.J., Guzik, J.A., Bradley, P.A., Cox, A.N., and Middleditch, J. 1997,

- AJ*, **114**, 1592.
- Udalski, A., Kubiak, M., Szymański, M., Kałużny, J., Mateo, M., and Krzeminski, W. 1994, *Acta Astron.*, **44**, 317.
- Udalski, A., Szymański, M., Kałużny, J., Kubiak, M., Mateo, M., and Krzeminski, W. 1995a, *Acta Astron.*, **45**, 1.
- Udalski, A., Olech, A., Szymański, M., Kałużny, J., Kubiak, M., Mateo, M., and Krzeminski, W. 1995b, *Acta Astron.*, **45**, 433.
- Udalski, A., Olech, A., Szymański, M., Kałużny, J., Kubiak, M., Krzeminski, W., Mateo, M., and Stanek, K.Z. 1996, *Acta Astron.*, **46**, 51.
- Udalski, A., Olech, A., Szymański, M., Kałużny, J., Kubiak, M., Mateo, M., Krzeminski, W., and Stanek, K.Z. 1997, *Acta Astron.*, **47**, 1.
- Udalski, A., Szymański, M.K., and Szymański, G. 2015, *Acta Astron.*, **65**, 1.
- Walker, M.F. 1952, *PASP*, **64**, 192.
- Watson, C.L., Henden, A.A., and Price, A. 2006, *Soc. Astron. Sci. Annu. Symp.*, **25**, 47.
- Woźniak, P.R. 2000, *Acta Astron.*, **50**, 421.
- Zloczewski, K., Kaluzny, J., Rozyczka, M., Krzeminski, W., and Mazur, B. 2012, *Acta Astron.*, **62**, 357.